High Brightness kW QCW Diode Laser Stacks with Ultra-low Pitches

David Schleuning*, Rajiv Pathak, Calvin Luong, Eli Weiss, and Tom Hasenberg
*Coherent Inc., 5100 Patrick Henry Drive, Santa Clara, CA 95054

ABSTRACT

State-of-the-art QCW solid-state lasers are demanding ever higher brightness from the pump source—conduction cooled diode laser stacks. The intensity of a QCW vertical stack is limited by the peak power of each diode bar and the bar pitch. The minimum bar pitch of the existing laser diode stacks on the market is about 400um. In this paper, we present a unique vertical diode laser stack package design to achieve a bar pitch as low as 150um, which improves the intensity of the stack by nearly 3 times. Together with the state-of-art diode laser bar from Coherent, greater than 30kW/cm^2 peak power density is achieved from the emitting area of the vertical stack. The p-n junction temperature of the diode bars in the device under QCW operation is modeled with FEA software, as well as measured in this research. Updated reliability results for these diode laser stacks are also reported.

Keywords: semiconductor laser diodes, packaging, material properties

1. INTRODUCTION

Semiconductor laser bars on conduction cooled platforms have a number of industrial applications. Primarily conduction-cooled stacks are used to pump Q-switched solid state lasers and therefore can be operated in Quasi-CW mode with pulse widths on the order of the upper state lifetime of the gain medium and with repetition rates as needed for the application.

To achieve higher intensity (kW/cm^2) for a stack one can: (1) increase the power/bar or (2) decrease the pitch between bars. In both approaches the increased heat density should increase both the transient temperature (chirp) as well as the equilibrium temperature due to the average heating. However, there are a number of applications that only require low duty cycles (<1%) and reliability targets of hundreds of Mshots. Therefore an appropriate tradeoff for higher performance can be made. In our approach we decrease the pitch between the bars used the standard G-stack configuration. We use FEA modeling and measurements to quantify the temperature response. With a detailed model of the transient and an average heating in the stack we demonstrate the ability to produce a wide-bandwidth stack with ~8nm of tuning range. Finally we combine the two approaches by increasing power/emitter and reducing the pitch to demonstrate a high intensity device in a small form-factor package.

2. HIGH DENSITY STACK

The figure below shows an example of a traditional G-stack with 400 um pitch compared to a high density stack with 150 um pitch. The bars have a 90% fill-factor, 1.5mm cavity length and fast axis divergence of 23 degrees. The traditional G-stack uses AuSn bonding of the p-side die to CuW rails and a BeO insulating plate (details given in ref [1]). This stack can be configured to hold 2 to 7 bars that are connected electrically in series; the results in this paper will show 7 bar stack results with 200W/bar.

The high density stack (on the right) uses an all AuSn attachment of the bars to end caps that act as heat spreading rails. This design can easily be configured to use a different number of bars. The heat spreading rails are connected to an insulating plate and then to a copper base heat sink. The copper base for both designs is identical with the same dimensions and hole pattern. The electro-optical results below compare the same bar design on 6 bar high density stacks.

High-Power Diode Laser Technology and Applications VII, edited by Mark S. Zediker,
Proc. of SPIE Vol. 7198, 719802 · © 2009 SPIE · CCC code: 0277-786X/09/$18 · doi: 10.1117/12.809637

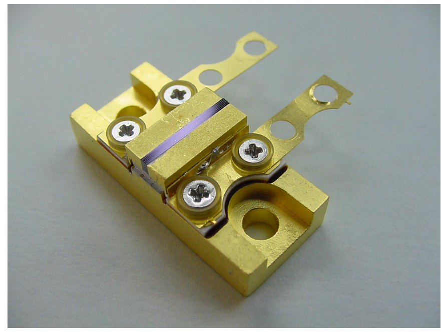

Fig. 1. A traditional G-stack (400um pitch) compared to a high density stack (150um) pitch

The figure below shows the P-I curve comparing a traditional G-stack to a high-density stack. Both are measured with a 250 uSec pulse width and a frequency of 40 Hz giving a duty cycle of 1%. The results are converted to power/bar since the traditional stack was fabricated with 7 bars while the high density stack was made with 6 bars. The high density stack shows a slightly degraded performance at high power which results in <10A difference in operational current at 200W/bar power levels.

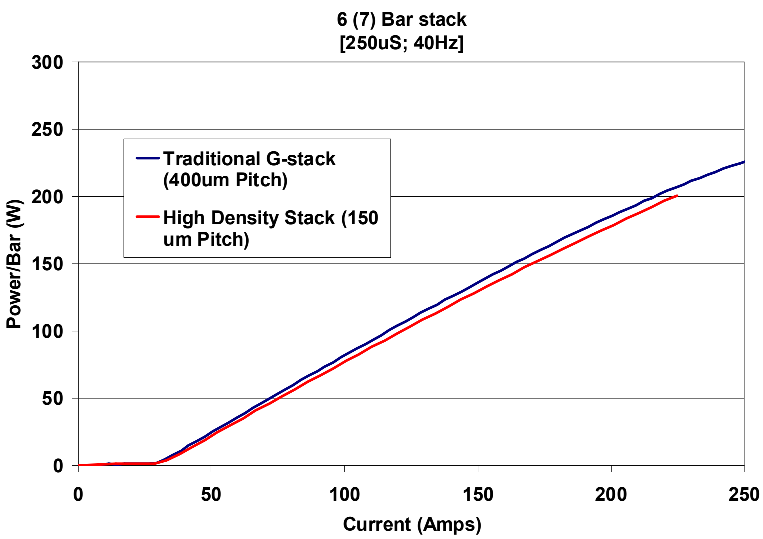

Fig. 2. Power/bar vs. current for a G-stack with 400 μm pitch (7 bars) compared to a high density stack with 150 μm pitch (6 bars).

3. THERMAL MODELING

In a conventional conduction cooled stack (G-stack) the thermal resistance is too high to run in CW mode and is typically operated in pulsed (QCW) mode. Therefore the junction temperatures of the diodes in the stack are increased from the baseplate temperature by two effects: (1) the transient temperature—often called "chirp" and (2) the average temperature—determined by the thermal resistance and the heat load.

3.1 Temperature-Wavelength Dependence

To determine the temperature dependence of a stack we calibrate individual stacks by measuring the wavelength at various heatsink temperatures under low duty cycle conditions. In all measurements the conduction cooled stack is mounted to a water-cooled plate. The temperatures below are obtained by changing the water temperature flowing through the heatsink and measuring the temperature on the copper baseplate of the stack. We note that the heatsink temperature is typically a few degrees lower than the water temperature as measured by the chiller/heater at higher temperatures leading to lower dλ/dT values than if one relies on the water temperature to determine dλ/dT.

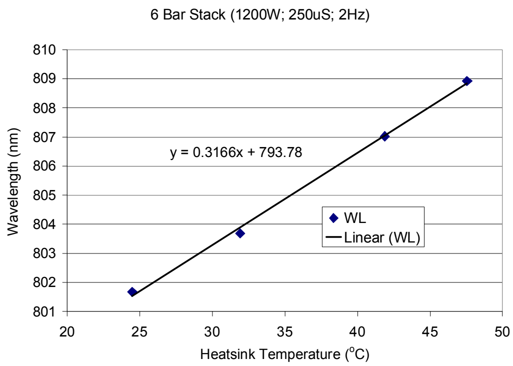

Fig. 3. Centroid wavelength vs. temperature for a high-density stack.

3.2 Transient Properties

To model the transient properties of a high-density stack we use a FEA study of the stack by assuming that all of the heat is generated on the P-side of the GaAs chip during a 250 µSec pulse. Since heat flow is constrained by the geometry of the package and since these stacks use a 90% fill-factor bars we use a 2 dimensional approximation to ease the computational analysis. In the figure below we show the temperature distribution of a 6 bar high density stack at time steps of 50, 150 and 250 µSec under a 200W heat pulse. The temperature distribution along the cavity length of a laser (vertical in the figure) shows a very uniform temperature distribution.

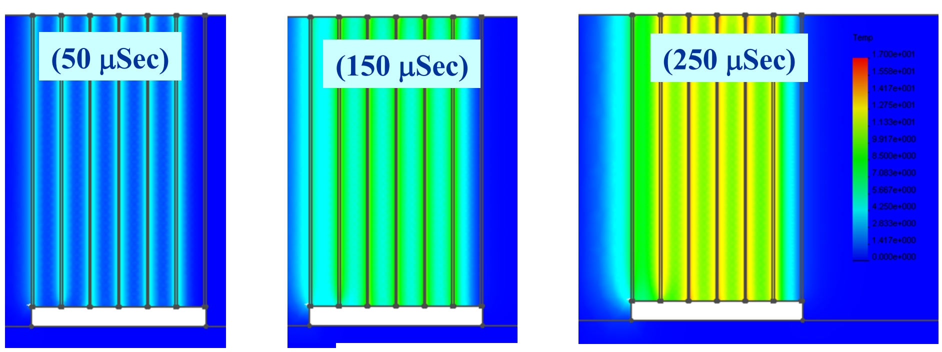

Fig. 4. Finite element analysis of the transient temperature response for a high density stack with 200 W/bar (heat) for a 250 uSec pulse. Temperature distributions are shown across the profile of the stack (i.e. light emission is upward in this orientation) for 50, 100, and 150 µSec time steps.

In the figure below, the time temperature curves (left) are shown for each bar in the stack. Bar#5—the right-most bar soldered directly to the end cap—has the lowest transient temperature performance heating up by ~8 degrees. The central bars heat up the most with max temperatures of ~17 degrees. To synthesize the expected output spectrum of the stack, we consider the contributions of all the time steps and of all the bars, and then convert the temperature distribution using the dL/dT relationship determined above. The predicted spectrum from this semi-empirical model is shown in the lower right below and predicts a wavelength shift of 2.6nm with a standard deviation of 1.2 nm.

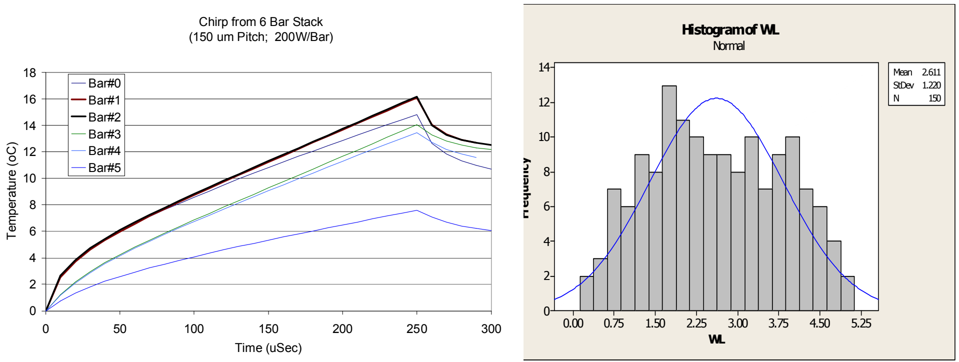

Fig. 5. The time-temperature response for each bar in the stack for a 250 µSec pulse (200W/bar). The histogram on the right shows the distribution of wavelengths (converted from temperature) for all of the bars integrated over the 250 µSec pulse.

In the figure below we show the measured results for a high-density stack under different peak power conditions; all of the data has the same 250uS pulse width with a low duty cycle of 0.05% (2 Hz). The left-most spectrum shows the effect of low transient heating with low power of 150W (25 W/bar). The 6 bars in stack are well wavelength matched and have low residual packaging stress to give a spectral width of ~1nm. As the power is increased to 600W (100W/bar) and 1200 W (200W/bar) one can see two effects: (1) the centroid wavelength is red-shifted or "chirped" and (2) the spectral width is broadened. The broadening occurs because the increased heat causes an increased temperature (wavelength) spread in time for each bar. In the right-hand plot we show the measured centroid wavelength and the error bars show the FWHM of the spectrum.

To compare the FEA model to the data we make the following assumptions: (1) the optical power is converted to dissipated heat using the measured WPE efficiency; (2) the temperature for each bar is integrated over time; (3) the temperature for all the bars are integrated together; (4) the temperature distribution is converted to wavelength by the empirically determined values of λ_o and $d\lambda/dT$. The predicted results from the FEA model (solid line in figure below) show excellent agreement to the measured data. The upper limit (dashed line) is the hottest bar plus the HWHM of its time integrated spectrum. The lower limit (dotted line) is the coldest bar minus the HWHM of its time integrated spectrum. Note: the lines do not try to fit the data; rather the only fit parameters in this model are the offset wavelength λ_o and $d\lambda/dT$. In sum, the transient chirp for this device is ~10 ^{o}C and the results can be well modeled and therefore predicted for other pulse conditions or stack geometries (i.e. different λ_o for each bar in the stack)

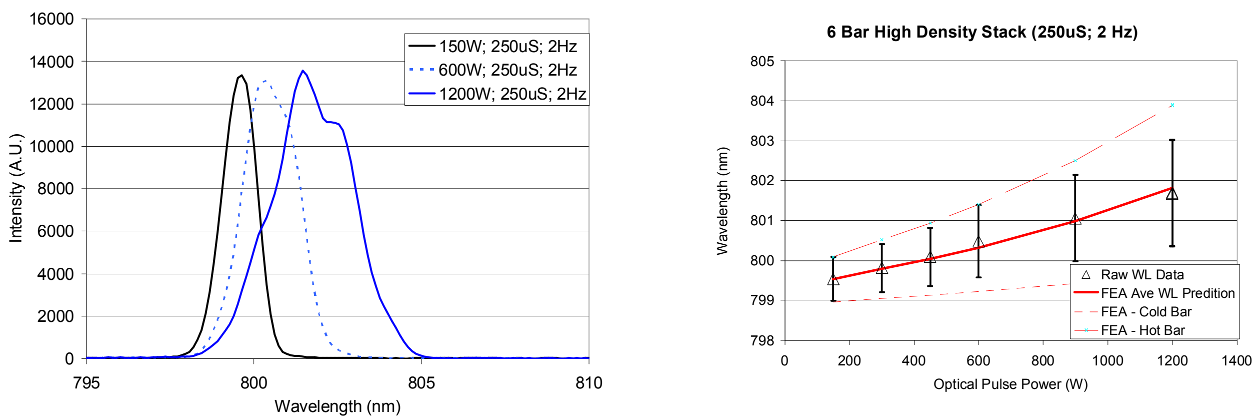

Fig. 6. (a) Spectral response for a high-density stack under low duty cycle pulse conditions of 250uS at 2Hz with different peak powers. (b) The black triangles give the measured centroid wavelength and error bars show the spectral width (FWHM). The lines show the predicted wavelength shift and spectral width from the FEA model.

3.3 Thermal Resistance

In addition to the transient temperature rise due to each QCW pulse, there is an average heating component, which corresponds to the heat load times the duty cycle. We analyze this effect with a 3-dimensional FEA model shown in the figure below. Compared to the traditional 400 um pitch G-stack, the high density stack has an increased temperature and a larger temperature gradient with the hottest bars in the center. However, similar to the transient model there is a lower temperature gradient along the cavity length direction for each laser compared to the traditional Gstack.

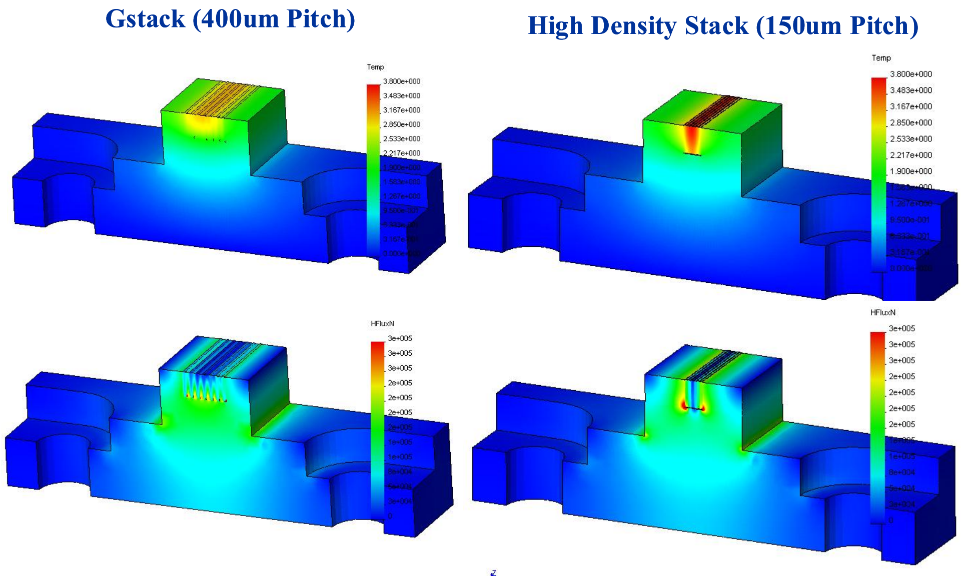

Fig. 7. Finite element analysis of the steady state thermal response with a 1 W/bar heat load for (a) a traditional G-stack with a 400 um pitch (left) and (b) a high density stack with150um pitch (right). Upper pictures show the temperature distribution (^{o}C); the lower pictures show the heat flux (W/m^2).

Under higher duty cycle conditions the average heat load will heat all of the lasers red-shifting the spectral distribution. In addition, the temperature gradient—from the center to the outer bars—will broaden the spectrum. In the figure below we show the spectral characteristics under low duty cycle conditions of 0.05% (2Hz) compared to the effects with higher duty cycle 1% (40 Hz). In the right plot below we show this trend over a series of frequencies to show the average heating effects up to 80 Hz repetition rates.

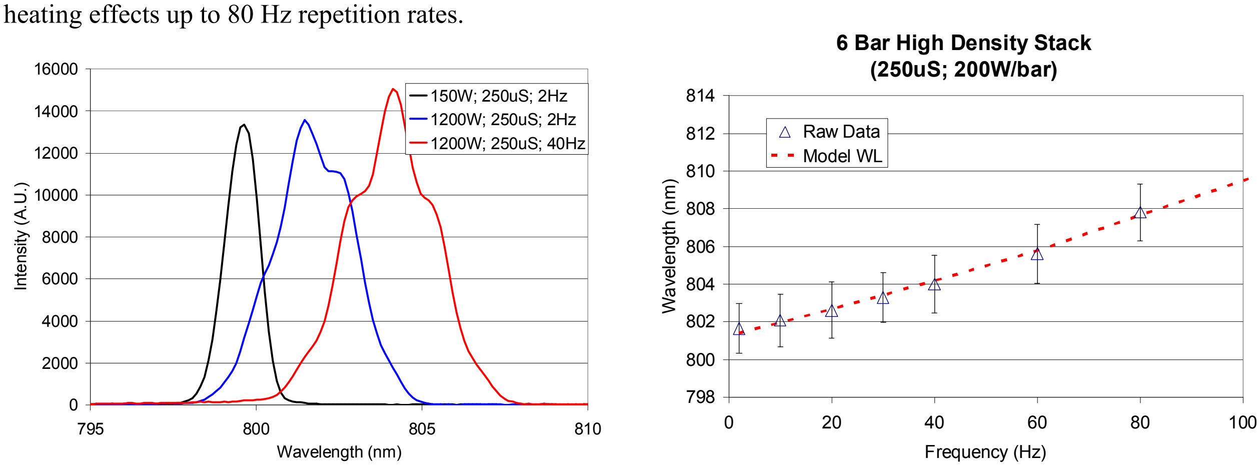

Fig. 8. (a) Wavelength spectrum under different QCW conditions. (b) Wavelength response to increasing the frequency (or duty cycle) for fixed pulse width and peak power; The black triangles give the measured centroid wavelength and error bars show the spectral width (FWHM). The dashed line is fit to the data.

4. RELIABILITY

We have performed a limited lifetest on two high-density stacks (150 µm pitch) and one traditional stack (400 µm pitch). In the figure below the devices show stable power through greater than 50 Mshots (220A; 250uSec pulse width; 1% duty cycle). Although this data set is limited, the temperature performance determined above combined with previous reliability studies some indication that these stack will achieve >100 Mshots and potentially Gshots of reliability.

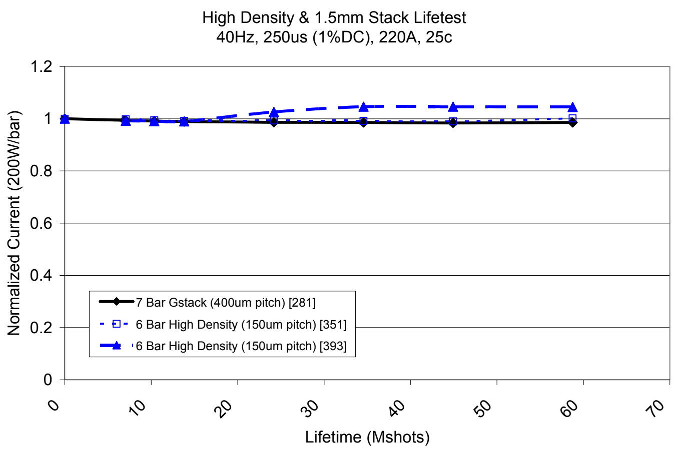

Fig. 9. Reliability of high-density stacks compared with a traditional G-stack under QCW conditions (~200W/bar; 250 µSec pulse width; 40 Hz [1% duty cycle]; 25°C).

5. MULTI-WAVELENGTH HIGH DENSITY STACK

The figure below shows the power-current performance and wavelength spectrum for a high-density stack (150 um pitch) made with bars separated into well-defined wavelength bins (~3nm spacing). For this design we used high efficiency bars with a 90% fill-factor, 1.0mm cavity length and fast-axis divergence of 31 degrees. The stack achieves 1200 W (200 watts/bar) of peak power with a 1% duty cycle at a current of ~190A. We have designed the stack to have a blended spectral response to give a ~8nm bandwidth which is desirable for pump applications that require loose temperature control. In the figure on the right, we demonstrate the ability to select and bin bars with good precision to match pairs of bars to less than <.5nm and then separate the pairs by ~3 nm. Increasing the pulse width (similar to increasing the power above) shows the effect blending the spectral response due to the transient ("chirp") temperature response. Increasing the duty cycle, adds the average heating component, which spreads the spectrum into six well-identified peaks at the operating condition of 200 W/bar at 250 uSec at 40 Hz. The final operational spectrum has a 8nm bandwidth which will provide an effective pump source over a broad temperature range.

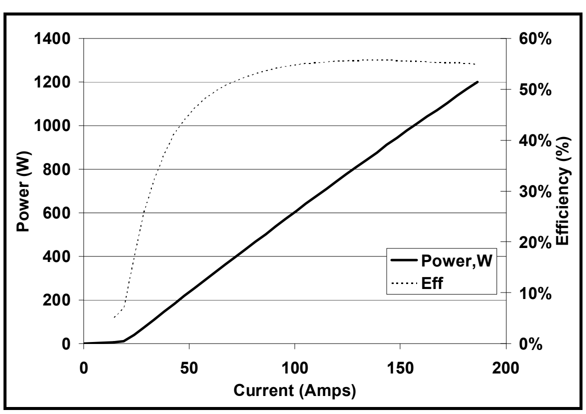

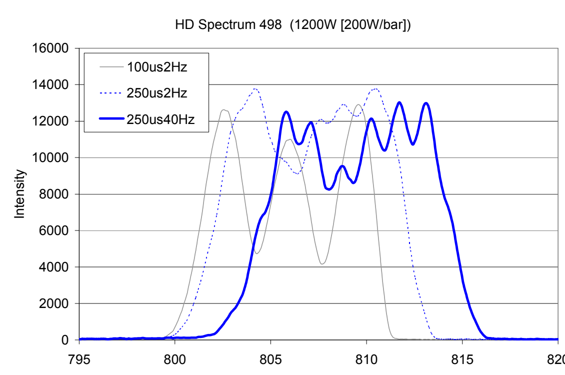

Fig. 10. Results for a 6-bar high-density (150 um pitch) stack made with bars from three wavelength bins that are separated by ~3nm. (a) Power-current and efficiency curves. (b) Spectral response under different QCW pulse conditions.

6. SMALL FORM FACTOR STACKS

To further increase the brightness and incorporate a small form factor package, we have designed and built a small mini-bar (3mm width) with higher facet power capability. This chip is mounted in a high density stack configuration with 2 mini-bars separated by a 150 um pitch. At low duty cycles this device is capable of reaching 150 W with an intensity of >30 kW/cm^2. The figure below shows the L-I characteristics of this device at low duty cycle. On the right we show a picture of the small form-factor device with fast-axis collimation compared to the size of a dime. We note that the mini-stack used a 31deg divergence chip design; however, lower divergence epi design is fully compatible with this packaging platform and thus a further increase in brightness is possible.

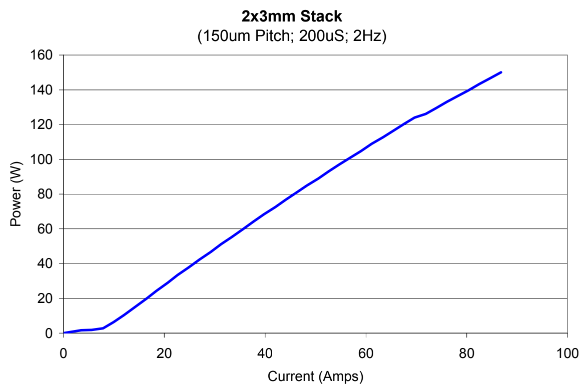

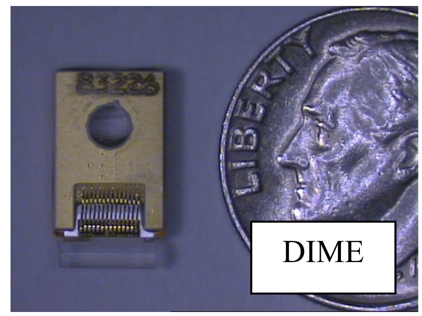

Fig. 11. (a) Power-current curve for a small form factor stack. (b) Picture of a small form-factor stack with fast axis collimation compared to the size of a dime.

Table. 1. Summary of the parameters for the intensity and brightness of the stacks presented in this paper.

Design	width [mm]	pitch [□m]	Bars	P/Bar [W]	Power [W]	FA div [deg]	SA div [deg]	Intensity [kW/cm^2]	Brightness [kW/cm^2/Str]
Std G-stack	10	400	7	200	1400	31	10	5.8	247
HB stack	10	150	6	200	1200	23	10	16.0	913
Mini-Stack	3	150	2	75	150	31	10	33.3	1412

7. CONCLUSIONS

In the table above, we summarize the parameters of the stacks described in this paper. We have demonstrated high density stacks with reduced pitch and lower fast axis divergence, which have increased the brightness by a factor of 3. We presented a detailed thermal model which accurately predicts the transient and average temperature response of each bar in the stack to different pulse conditions. Using this capability we have designed a demonstrated a wide bandwidth (8nm) stack capable of pumping over a wide temperature range. High density stacks with 150um pitch (200 W/bar; 250uS; 1% duty cycle) have demonstrated >50 Mshots of lifetest without degradation. Finally we have presented a small form-factor package that utilizes the high-density stack concept and is capable of 150 W with high intensity for low duty cycle applications. The mini-stack has the highest intensity by utilizing increased power per emitter and reduced the pitch between bars.

REFERENCES

[1] Rosenberg et al., "Highly reliable hard soldered QCW laser diode stack packaging platform", High-Power Diode Laser Technology and Applications V, Proc SPIE Vol 6456-18, 2007.

[2] Du et al., "8xx nm kW Conduction Cooled QCW diode arrays with both electrically conductive and insulating submounts", High-Power Diode Laser Technology and Applications VI, Proc SPIE, 2008.

[3] McNulty, J. "Processing and Reliability Issues for Eutectic AuSn Solder Joints", IMAPS, 2008